

Using wavelets to analyze similarities in image datasets

Roozbeh Yousefzadeh

Depts. of Genetics and Computer Science
Yale University, New Haven, CT
roozbeh.yousefzadeh@yale.edu

Abstract

Deep learning image classifiers usually rely on huge training sets and their training process can be described as learning the similarities and differences among training images. But, images in large training sets are not usually studied from this perspective and fine-level similarities and differences among images is usually overlooked. Some studies aim to identify the influential and redundant training images, but such methods require a model that is already trained on the entire training set. Here, we show that analyzing the contents of large training sets can provide valuable insights about the classification task at hand, prior to training a model on them. We use wavelet decomposition of images and other image processing tools to perform such analysis, with no need for a pre-trained model. This makes the analysis of training sets, straightforward and fast. We show that similar images in standard datasets (such as CIFAR) can be identified in a few seconds, a significant speed-up compared to alternative methods in the literature. We also show that similarities between training and testing images may explain the generalization of models and their mistakes. Finally, we investigate the similarities between images in relation to decision boundaries of a trained model.

of models on testing sets and understand their misclassifications in relation to training sets. Some studies in the literature aim to identify redundant and influential images in datasets. However, such analysis is performed in a post-hoc way and require a model that is trained on all the data. Here, we provide tools to directly analyze images prior to training, and show that valuable insights can be gained from such analysis.

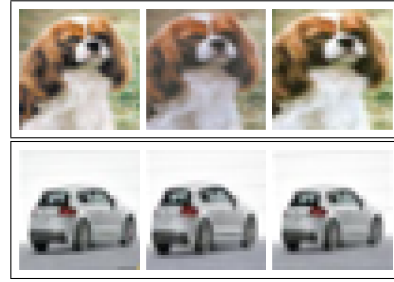


Figure 1: Example of nearly identical images in CIFAR-10 training set.

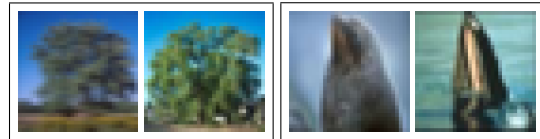


Figure 2: Example of similar images with different labels in CIFAR-100 training set: oak and maple tree (left), whale and seal (right).

1 Introduction

Studying the similarities and differences among images in training sets may provide valuable insights about the data and the models trained on them. For example, we may identify redundancies and/or anomalies in the training sets, or we may gain insights about the generalization

Figure 1 shows examples of redundancies present in the CIFAR-10 dataset and Figure 2 shows examples of similar images with different labels in the CIFAR-100 dataset. We provide a method to identify all of such similarities in a few seconds, with no need for a trained model.

1.1 Image classifiers and their decision boundaries

Any classification model is defined by its decision boundaries, and hence, training process of a model can be viewed as defining those decision boundaries for the model [Fawzi et al., 2018]. Consider for example, the case of training a linear regression model. What happens during the training is basically defining the location of the regression line (i.e., decision boundary) to partition the input space. Training of an image classification model is also partitioning its input space, although such partitions can be geometrically complex in the high dimensional space.

From this perspective, any training image that does not affect the decision boundaries of a model can be considered redundant, and any training image that causes a decision boundary to be defined in the input space can be considered influential. Therefore, when a group of images from the same class are similar, it is likely that only one of them would suffice to define the necessary decision boundary in that neighborhood in the domain.

On the other hand, when images of different class are similar (e.g., see Figure 2), all of them would be influential, because they are similar, and learning them would cause the model to define the necessary decision boundaries between them. We study these conjectures in our numerical experiments.¹

1.2 Our plan

We propose two methods to analyze the similarities among images in a dataset. The first method is fast and effective to identify similar images. The second method performs a thorough analysis of images using specialized image processing tools. We show the effectiveness of our methods on standard object recognition datasets such as CIFAR-10 and CIFAR-100 [Krizhevsky et al., 2009], and also one class of Google Landmarks dataset [Noh et al., 2017].

In Section 2, we review the related work. In Sections 3 and 4, we describe each of our methods, respectively. Section 5 includes our numerical results. Finally, in Section 6, we discuss our conclusions and directions for future research.

¹As in most machine learning tasks, the underlying assumption is that the data in the testing set generally comes from a similar distribution as the training set and learning the similarities and differences among images in the training set is the key to achieving good generalization.

2 Related work

One of the early studies in the literature is by Ohno-Machado et al. [1998] which reports existence of redundancies in medical training sets, but their computational method is not practical for modern applications of deep learning.

There are studies that measure the influence of training points based on the derivatives of the loss function of a trained model. Guo and Schuurmans [2008] studied the derivatives of mini-batches to select subsets of unlabeled data but their method is specific to active learning, where there is a stream of new training data. Vodrahalli et al. [2018] showed that choosing training images with most diversity of derivatives can speed up the training, but their analysis is based on models trained on all the data. Recently, Sankararaman et al. [2019] explained the speed of training in terms of correlation between gradients.

There are also methods that consider the value of loss function or norm of gradients [Loshchilov and Hutter, 2015, Alain et al., 2015, Katharopoulos and Fleuret, 2018]. Such measures are useful to speed up the training, but not necessarily meaningful proxies to compare similarity of images. Additionally, since they require computation of loss and gradient of a model, they are more expensive than direct comparison of images using image processing tools.

Lapedriza et al. [2013] proposed a greedy method to sort the data points in training sets based on their importance for training. For the sorting, they define a “training value” which requires the model to be separately trained from scratch for each training image.

Influence functions have been used to quantify the effect of individual training data on a trained model [Koh and Liang, 2017, Koh et al., 2019], but the assessment of influence requires a model trained on all the data.

Carlini et al. [2018] developed a method that first projects the images from the pixel space into a two dimensional space, and then performs clustering in the low dimensional space, but the projection requires a model trained on all the training set.

There are other studies focused on interpretability of image classification models that make use of prototypes, for example, Kim et al. [2014], Li et al. [2018], Chen et al. [2019]. Such methods aim to train a model such that its output is explainable in terms of similarity to prototypes. To compare an image with a prototype, Chen et al. [2019] inverts the ℓ_2 norm distance between the output of a trained convolutional layer and the prototype.

Meletis et al. [2019] used a Gaussian Mixture Model (GMM) to identify visually similar images using a pre-trained model.

Birodkar et al. [2019] used clustering of images in a semantic space to identify redundant images. The semantic space in their study is the intermediate output of a trained model. Barz and Denzler [2019] also showed that redundant images in CIFAR datasets can be identified using the output of an average pooling layer.

Chitta et al. [2019] showed that a portion of some training sets can be removed leading to no loss of accuracy. Their method trains an ensemble of deep neural networks on all the training set in order to identify such redundancies. Yousefzadeh and O’Leary [2019a] showed that the distance of training images to the decision boundaries of a trained model can identify the most influential training data.

All the approaches above identify the influence of training images through the lens of a model that is trained on all the data. Here, we show that using wavelets, one can analyze the images and obtain valuable information about them, before engaging in the training process.

Achille et al. [2019] studied the similarities between different image classification tasks, e.g., classifying different kinds of birds vs different kinds of mammals, which can provide valuable information about the nature of those classification tasks, however, their approach requires model training.

Finally, we note that there are unsupervised methods that aim to create an embedding for groups of images. For example, Vo et al. [2019] solves an optimization problem for each image pair to measure their similarity and then creates an embedding based on that information. However, such methods are not scalable to analyze an entire training set.

3 Finding similar (redundant and influential) images in the data

Here, we develop a simple and fast algorithm to identify similar images in training sets. Our algorithm first decompose the images using wavelets, then chooses a subset of wavelet coefficients that have the most variation among images. Finally, it clusters the images based on their wavelet coefficients. Images that are similar will appear in same clusters and that would lead to identifying influential and redundant images.

3.1 Wavelet decomposition of images

We use the wavelet transformation of images as a mean to identify similar training data. Wavelets are a class of functions that have shown to be very effective in analyzing different kinds of data, especially images and signals. Wavelets can also be used to analyze functions and operators [Daubechies, 1992]. In both image processing and signal processing, wavelets have been effective in compressing the data and also in identifying actual data from the noise [Chui, 2016].

The main idea here is to decompose each image into different frequency components and then analyze the components among the images to identify their similarities and differences. Wavelets allow us to analyze images at different resolutions and therefore enable us to compare them effectively.

Decomposing an image using a wavelet basis is basically convolving the wavelet basis over the image. This is similar to the operation performed by convolutional neural networks. Therefore, our method of analyzing and comparing images is similar to the computational method that will be used by the classification models.

In this paper we use wavelets, but we note that shearlets [Kutyniok and Labate, 2012] are also a class of functions with great success in analyzing images, and therefore they can be considered instead of wavelets.

3.2 Extracting a subset of influential wavelet coefficients

We are interested in the similarities and differences among subgroups of images. But, as we will show in our numerical experiments, many of the wavelet coefficients can be similar among all images in a training set and therefore, not helpful for our analysis.

When computing wavelet decomposition, one can use different resolutions to convolve the wavelet basis with images. Since we are concerned with the overall similarity of images, there will be no need to extract the wavelet coefficients on a very fine level. Therefore, even for relatively large images in Imagenet and Google Landmarks datasets, one can extract a relatively small number of wavelet coefficients by convolving the images with high pass filters.

Once we have computed the wavelet coefficients for images, we use rank-revealing QR factorization [Chan, 1987] to choose a subset of coefficients that are most linearly independent among the images. Rank-revealing QR algorithm and also its variation, pivoted QR algorithm [Golub and Van Loan, 2012] decompose a matrix by computing a column permutation and a QR factoriza-

tion of a given matrix. The permutation matrix orders the columns of the matrix such that the most linearly independent (non-redundant) columns are moved to the left. The rows of our matrix represent the images and its columns represent wavelet coefficients.

The obtained permutation matrix allows us to choose a subset of most independent columns. This dimensionality reduction in the wavelet space, previously used by Yousefzadeh and O’Leary [2019b,c], can make our next computational step (i.e., clustering) faster.

As an example, consider the 60,000 images in the training set of MNIST dataset. Each image has 784 pixels, leading to 784 wavelet coefficients using the Haar wavelet basis. 32 of those wavelet coefficients are 0 for all images. After discarding those coefficients, the condition number of the training set is greater than 10^{22} , implying linear dependency of columns. After performing rank-revealing QR factorization, we observe that dropping the last 200 columns in the permutation matrix will decrease the condition number to about 10^6 . All the discarded features will be completely unhelpful in identifying influential and redundant data, because they are either uniform or (almost) linearly dependent among all images.

The cost of computing the rank-revealing QR factorization is $\mathcal{O}(nd^2)$ given n images with d wavelet coefficients [Golub and Van Loan, 2012]. We would not need to compute the entire decomposition as the computation can be stopped as soon as a diagonal element of R becomes small enough compared to its first diagonal element.

The computational cost of clustering, however, can be higher. For example, if we use k-means, the cost can be $\mathcal{O}(ndkl)$, where k is the number of clusters and l is the number of clustering iterations. We expect the number of clusters to be proportional to n , with a constant factor less than 1. Hence, the cost of computing rank-revealing QR decomposition can be smaller than clustering, and it would be beneficial to perform the clustering on the influential wavelet coefficients (chosen by the rank-revealing QR algorithm).

3.3 Clustering images based on their wavelet decomposition

Any clustering method can be utilized to cluster the images based on their wavelet coefficients. We use k-means clustering [Lloyd, 1982, Arthur and Vassilvitskii, 2007] in our numerical results. The computational effort for clustering depends on the number of observations (size of training set) and also the number of features considered for each image. We suggest performing the cluster-

ing on the entire dataset (when possible), noting that it will be a more expensive computation compared to clustering images of each class, separately. Clustering per class would cost less, but would not provide the additional insight about influential images.

3.4 Our algorithm based on wavelet coefficients and clustering

Algorithm 1 formalizes the above process in detail.

Algorithm 1 Algorithm for finding similar training images using wavelet coefficients and clustering

Inputs: Training set \mathcal{D}^{tr} , τ , n_c

Outputs: Reduced training set $\hat{\mathcal{D}}^{tr}$

- 1: Count number of images in \mathcal{D}^{tr} as n
 - 2: **for** $i = 1$ to n **do**
 - 3: Compute wavelet coefficients of image i , vectorize them and save them in row i of matrix W
 - 4: **end for**
 - 5: **if** $n >$ number of wavelet coefficients per image **then**
 - 6: $[Q, R, P] = \text{RR-QR}(W)$, i.e. perform rank-revealing QR on W
 - 7: Choose m as large as possible such that the first m columns of the matrix WP has condition number less than τ
 - 8: Extract the first m columns of WP and save it as \hat{W}
 - 9: **end if**
 - 10: Perform clustering on \hat{W} with n_c clusters
 - 11: **for** $i = 1$ to n_c **do**
 - 12: **if** there are more than one image in cluster i and all images in the cluster are from the same class **then**
 - 13: Keep the image closest to the center of that cluster and discard other images in cluster
 - 14: **end if**
 - 15: **end for**
 - 16: Put together remaining images in clusters as $\hat{\mathcal{D}}^{tr}$
 - 17: **return** $\hat{\mathcal{D}}^{tr}$
-

The algorithm first computes wavelet decomposition of all images in the training set and forms them in a matrix W , where rows are samples and columns are wavelet coefficients (lines 1 through 4). The next step in the algorithm is to compute the rank-revealing QR factorization of W (line 5). This factorization computes an orthogonal matrix Q , an upper-triangular matrix R , and a permutation matrix P , such that

$$WP = QR.$$

Algorithm 1 then chooses a subset of m most indepen-

dent wavelet coefficients according to the permutation matrix (lines 6 and 7). The condition for choosing m is to maximize its value such that the condition number of the first m columns of WP is less than τ . For a given dataset, this condition will yield a unique value for m . The best value for τ could vary based on the properties of the dataset. The trade-off here is that choosing a small τ will yield a small m , making the clustering computation less expensive, while using a very small m may not be able to adequately capture the variations among images and lead to poor results. In our numerical experiments, we found $\tau = 10^5$ to be a good choice.

The final stage of the algorithm is to perform clustering and to discard the redundant images from each cluster (lines 9 through 13).

About the number of clusters, n_c , its best value would depend on the portion of redundancies in a training set which is likely to be unknown. One can choose an adaptive clustering method to find the right n_c . Alternatively, one can build a similarity matrix and investigate the eigen-gaps of graph Laplacian derived from that similarity matrix, which will be explained later.

4 Comparing images using specialized image processing tools

Algorithms 1 computes the wavelet decomposition of images and compares the images based on the similarity of their wavelet coefficients in the Euclidean space. We show in our results that this is adequate for identifying similar images in standard datasets for object recognition. However, we note that there are more sophisticated methods to compare images which we consider in this section.

4.1 Wavelet-based similarity measure between images

There are many methods in the image processing literature for measuring the similarities between images, for example, Reisenhofer et al. [2018], Wang and Simoncelli [2005], Sampat et al. [2009]. Albanesi et al. [2018] recently proposed a class of metrics to measure the similarity between pairs of images. Here, we use a relatively recent and widely used method known as the Structural Similarity Index (SSIM), developed by Wang et al. [2004], which compares images based on local patterns of pixel intensities that have been normalized for luminance and contrast.

Some of these measures are designed to measure specific kinds of similarity, for example, structural similarity, perceptual similarity, textural similarity, etc. Considering

the structure of images and patterns of pixel intensities make the SSIM particularly useful for image classification of objects such as the ones in CIFAR and Imagenet datasets. We note that the similarity measure should be chosen based on the classification task at hand. For example, in classifying images of skin cancer [Tschandl et al., 2018], the textures present in images may be more influential in classifications, instead of the structure of images. In such case, a texture-based similarity measure such as [Zujovic et al., 2013] may be more effective than the SSIM.

4.2 Analyzing the similarities among images

It is possible to envision Algorithm 1 such that images are clustered while their similarity is measured using a function like SSIM. This will cost more because computing SSIM between images is more expensive than computing the Euclidean distance between wavelet coefficients.

It is also possible to perform a more thorough analysis of images by building a similarity matrix and analyzing it. Here, we develop Algorithm 2 to perform such analysis using a specialized similarity function and using a spectral clustering method on the similarity matrix.

4.3 Our algorithm for thorough analysis of similarities

For each image pair in a training set, we compute the SSIM between them, and form a similarity matrix, \mathcal{S} , incorporating the pairwise similarities (lines 3 through 7 in Algorithm 2).

After computing the \mathcal{S} , our algorithm computes the eigenvalues of its graph Laplacian (line 8). Laplacian is the matrix representation of a graph corresponding to the similarity matrix. Instead of computing the precise eigenvalues, one can compute an estimate to the distribution of eigenvalues, using a Lanczos-based method, e.g., the method developed by Dong et al. [2019]. The next step is to choose the number of clusters, n_c , based on the number of eigen-gaps of the graph Laplacian, as suggested by von Luxburg [2007] (line 9). These two lines of the algorithm can be skipped, if the user wants to use a specific n_c , for example based on prior knowledge about the data.

The algorithm then completes the spectral clustering. The process of discarding redundant training data is similar to Algorithm 1. Overall this approach has $\mathcal{O}(n^3)$ because of the spectral clustering.

A low-cost alternative to spectral clustering is to check for each image, whether there are any other images sim-

Algorithm 2 Algorithm for analyzing training images using a similarity matrix

Inputs: Training set \mathcal{D}^{tr} , threshold on eigen-gaps γ , similarity function \mathcal{F}

Outputs: Reduced training set $\hat{\mathcal{D}}^{tr}$ and the list of most influential images \mathcal{I}

```

1: Count number of images in  $\mathcal{D}^{tr}$  as  $n$ 
2: Initialize similarity matrix  $S_{n \times n}$  as matrix of zeros
3: for  $i = 1$  to  $n - 1$  do
4:   for  $j = i + 1$  to  $n$  do
5:      $S_{i,j} = S_{j,i} = \mathcal{F}(\text{image } i, \text{image } j)$ 
6:   end for
7: end for
8: Compute the eigenvalues of the graph Laplacian of  $S$ , or an estimate to the distribution of eigenvalues.
9: Count the eigen-gaps larger than  $\gamma$  and use it as  $n_c$ 
10: Complete the spectral clustering on  $S$  with  $n_c$ 
11: for  $i = 1$  to  $n_c$  do
12:   if there are more than one image in cluster  $i$  then
13:     if all images in the cluster are from the same class then
14:       Keep the image closest to the center of that cluster and discard other images
15:     else
16:       Add the images in the cluster to the list  $\mathcal{I}$ 
17:     end if
18:   end if
19: end for
20: Put together remaining images in clusters as  $\hat{\mathcal{D}}^{tr}$ 
21: return  $\hat{\mathcal{D}}^{tr}$  and  $\mathcal{I}$ 

```

ilar to it and keep only one image from each group of images that have SSIM larger than a threshold. This basically requires investigating individual rows in the upper triangular section of S . The complexity of such algorithm is $\mathcal{O}(n^2)$ which might be appealing for large training sets.

We note that SSIM can be used in conjunction with other clustering methods, for example, k-means, leading to $\mathcal{O}(n)$ cost. In such approach, larger similarity between an image pair will be interpreted as closer distance between them and vice versa.

For datasets with large images, it is possible to compress the images first and then perform the analysis. The effectiveness of such approach would depend on the contents of images in the dataset.

5 Numerical experiments

Here, we investigate the similarities in three datasets: CIFAR-10, CIFAR-100, and one class of Google Land-

marks dataset. The code implementing our methods will be available online.²

5.1 CIFAR-10 dataset

We use the 2D Daubechies wavelets to decompose all images in this datasets. The matrix of wavelet coefficients has 50,000 rows and 3,072 columns and its condition number is 21,618. We use all the wavelet coefficients, because the condition number of matrix is not very large.

Using Algorithm 1, we cluster the images with $n_c = 47,000$. Figure 3 shows images in some of the clusters with uniform label. One training image per each of these clusters can suffice for training as there is no significant difference between them.

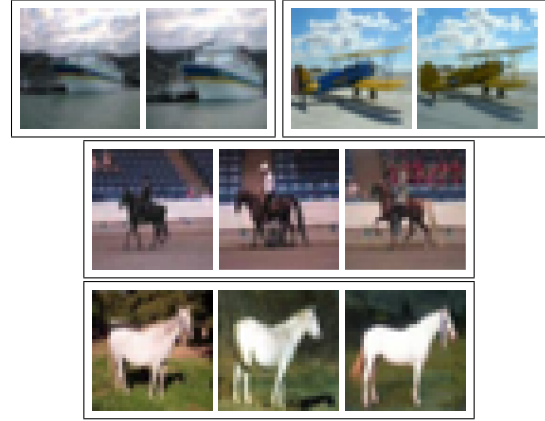


Figure 3: Example of similar images of same class in CIFAR-10 training set. Images in each box have formed one of the clusters. We see that a standard ResNet model does not have any decision boundaries between images of each group, while it has decision boundaries between dissimilar images of same class.

Birodkar et al. [2019] reported similar redundant training images in CIFAR-10 and showed that training a model without them does not adversely affect the accuracy of models on the testing set. Their method to identify the redundancies, however, requires training the ResNet model on the entire dataset, a process which can take a few GPU hours for the CIFAR-10 dataset. The advantage of our method is that it can efficiently identify the redundancies, prior to training. Since the redundancies we have found are similar to the redundancies identified by [Birodkar et al., 2019, Appendix], there is no need to repeat their experiments to measure the testing accuracy.

Figure 4 shows some of the same cluster images that have different labels. Clearly, it is desirable for a model to

²<https://github.com/roozbeh-yz/similarities>

learn these images and be able to distinguish them from each other.



Figure 4: Some of the similar images with different labels in CIFAR-10 training set. Each box shows one cluster. We consider these images influential in learning.

5.2 CIFAR-100 dataset

We identify redundancies in the CIFAR-100 training set, too, as briefly shown in Figure 5. Similar images with different labels are abundant in this dataset and might be even hard to distinguish for a human. For example, the image pair in the left box in Figure 2 represent a maple tree and an oak tree, and the image pair in the right box represent a whale and a seal.

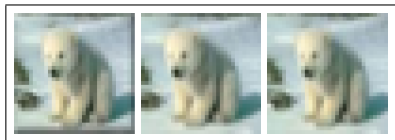


Figure 5: Example of redundant images in CIFAR-100 training set.

5.2.1 Class of aquarium fish (training set)

To gain more insight and to compare our algorithms, here, we consider only the second class of this dataset with 5,000 images.

Starting by Algorithm 1, the matrix of wavelet coefficients for this class is $5,000 \times 3,072$, with condition number 4×10^{18} . Numerical rank of this matrix is 495, using rank tolerance of $\tau = 10^{-5}$. We identify the 495 wavelet coefficients using rank-revealing QR factorization and use them for clustering with $n_c = 470$. The entire computation takes about 5 seconds on a machine with a 2.30GHz CPU and 115GB of RAM. We obtain redundant images as shown in Figure 6.

Let's see how the Algorithm 2 performs and what additional information it can provide. According to the SSIM measure, there are 5 pairs of identical images, all

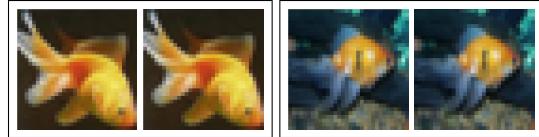


Figure 6: Example of redundant images in the aquarium fish class of CIFAR-100.

of which are also picked by Algorithm 1 (shown in Figure 6). In contrast, Figure 7 shows two of the most dissimilar image pairs based on the SSIM measure.

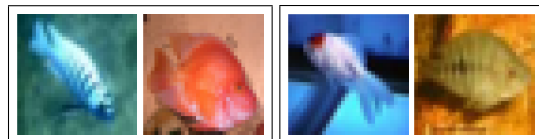


Figure 7: Two most dissimilar image pairs in the aquarium fish class of CIFAR-100, based on the SSIM measure. SSIM is -0.5420 for images in the left box and -0.5025 for the right box.

The mean value of the similarity matrix, S , is 0.088 and its standard deviation is 0.131. Figure 8 shows the distribution of eigenvalues of its graph Laplacian, implying that there are not any large clusters in the data. We choose the number of clusters based on the eigen-gaps of the graph Laplacian. Using the eigen-gap threshold as 0.4 leads to $n_c = 454$.

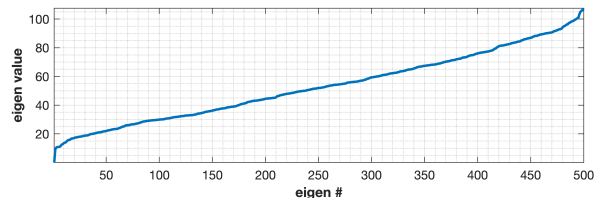


Figure 8: Distribution of eigenvalues of the graph Laplacian for all images in the “aquarium fish” class of CIFAR-100.

Spectral clustering then yields clusters with all the identical pairs mentioned above, with some additional images that are fairly similar, as two pairs are shown in Figure 9 because we chose a smaller n_c .

In summary, the results of our two algorithms corroborate each other. Algorithm 2 is more expensive for this example as expected, however, it provides more detailed insights about the images and guides us to choose a wise value for the number of clusters.



Figure 9: Examples of similar training images in CIFAR-100.

5.2.2 Class of aquarium fish (testing set)

We compare all 100 testing images of this class to all 500 training images of this class. The similarity matrix is shown in Figure 10. This analysis shows that 11% of testing images have a nearly identical image in training set. Figure 11 shows three testing images that have the least similarity to all images in the training set which happen to be common mistakes of classification models on CIFAR-100.

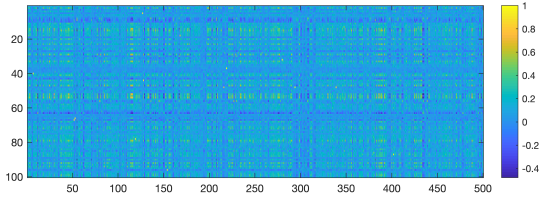


Figure 10: The similarity matrix between 100 testing images and 500 training images of the aquarium fish class in CIFAR-100.

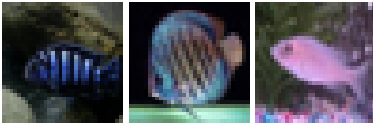


Figure 11: Testing images most dissimilar from the training set for the aquarium fish class. These happen to be common mistakes of standard models.

5.3 Influence of training data on decision boundaries of a trained model

We consider the standard ResNet-v2 models [He et al., 2016], pre-trained on CIFAR-10 and CIFAR-100 datasets and investigate their decision boundaries in relation to these images. A model’s decision boundary between two class is any point that produces equal softmax scores for those, while the softmax score for all other classes are less than those [Elsayed et al., 2018, Yousefzadeh and O’Leary, 2019a].

We aim to find whether the output of the model along the direct path connecting two images hits a decision bound-

ary or not. In other words, we want to find out whether the model has a decision boundary defined between two images. The direct path between two images \mathbf{x}_1 and \mathbf{x}_2 is defined by $(1 - \alpha)\mathbf{x}_1 + \alpha\mathbf{x}_2$, where α is a scalar between 0 and 1.

As expected, images that are almost identical in Figures 1, 5, and 6, do not have any decision boundary between them. On the other hand, images of the same class that are not similar do have decision boundaries between them, for example, images in Figure 7. This means that the model output along the direct path between such images exits the correct classification and re-enters it, hitting at least two decision boundaries in between. Interestingly, groups of images in Figures 3 and 9 that are similar but not identical, do not have any decision boundaries between them. This can be the subject of further study.

5.4 Google Landmarks dataset v2

For this dataset, we consider the class of Verrazzano-Narrows bridge. There are 56 images for this class which we standardized as 512 by 662 pixels. Using Algorithm 2, we analyze all training images in this class. Figure 12 shows the similarity matrix of images in the class and Figure 13 shows a graphical model derived from the similarity matrix.

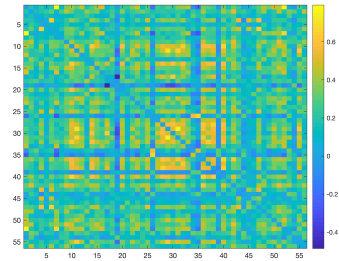


Figure 12: The similarity matrix for the class of Verrazzano-Narrows bridge in the Google Landmarks dataset v2.

Figure 14 shows the group of most similar images and Figure 15 shows the most dissimilar image pair in this class, according to the SSIM measure. Analyzing the similarity matrix reveals that the right image in Figure 15 is the most isolated image in the class.

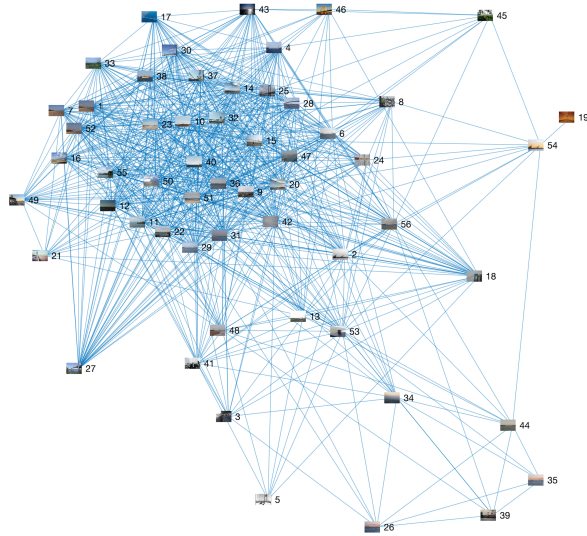


Figure 13: The graphical model derived from the similarity matrix.



Figure 14: Group of most similar images in the class (images 1,7, and 52 in the graphical model shown in Figure 13).

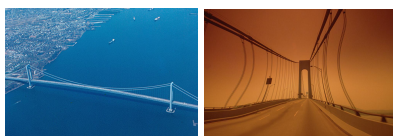


Figure 15: Most dissimilar images in the class of Verrazzano-Narrows bridge (images 17(left) and 19(right) in the graphical model). The image on the right is also the most isolated image in the class, based on the similarity matrix.

We note that our analysis has made us familiar with images in this class and provided us with insights about their similarities and differences. We know which training images might be redundant and which image might be an anomaly. In the case of active learning, we can try to fill the gaps in training data according to the graphical model shown in Figure 13.

6 Conclusions and future work

We developed a set of efficient tools for analyzing images in training sets. We showed that similar images in standard training sets can be identified efficiently and fast, prior to training a model on them. We showed that performing this types of analysis on training sets can provide useful insights about the data and also the models trained on them.

Possible extension of this work is to study the similarities and differences across training and testing sets and use that information to explain the generalization of models. Further investigating the images in relation to decision boundaries of models, during and after training, may provide useful insights about how training images shape the models. Moreover, our methods have applications in the context of active learning.

Acknowledgements

R.Y. is grateful to Dianne O’Leary for her helpful comments and advice.

References

- A. Achille, M. Lam, R. Tewari, A. Ravichandran, S. Maji, C. C. Fowlkes, S. Soatto, and P. Perona. Task2vec: Task embedding for meta-learning. In *Proceedings of the IEEE International Conference on Computer Vision*, pages 6430–6439, 2019.
- G. Alain, A. Lamb, C. Sankar, A. Courville, and Y. Bengio. Variance reduction in SGD by distributed importance sampling. *arXiv preprint arXiv:1511.06481*, 2015.
- M. G. Albanesi, R. Amadeo, S. Bertoluzza, and G. Maggi. A new class of wavelet-based metrics for image similarity assessment. *Journal of Mathematical Imaging and Vision*, 60(1):109–127, 2018.
- D. Arthur and S. Vassilvitskii. k-means++: The advantages of careful seeding. In *Proceedings of the 18th Annual ACM-SIAM Symposium on Discrete Algorithms*, pages 1027–1035, 2007.
- B. Barz and J. Denzler. Do we train on test data? purging cifar of near-duplicates. *arXiv preprint arXiv:1902.00423*, 2019.
- V. Birodgar, H. Mobahi, and S. Bengio. Semantic redundancies in image-classification datasets: The 10% you don’t need. *arXiv preprint arXiv:1901.11409*, 2019.
- N. Carlini, U. Erlingsson, and N. Papernot. Prototypical examples in deep learning: Metrics, characteristics, and utility, 2018.
- T. F. Chan. Rank revealing QR factorizations. *Linear Algebra and its Applications*, 88:67–82, 1987.
- C. Chen, O. Li, A. Barnett, J. Su, and C. Rudin. This

- looks like that: Deep learning for interpretable image recognition. *Advances in Neural Information Processing Systems*, 2019.
- K. Chitta, J. M. Alvarez, E. Haussmann, and C. Farabet. Less is more: An exploration of data redundancy with active dataset subsampling. *arXiv preprint arXiv:1905.12737*, 2019.
- C. K. Chui. *An introduction to wavelets*. Elsevier, 2016.
- I. Daubechies. *Ten Lectures on Wavelets*. Society for Industrial and Applied Mathematics, Philadelphia, 1992.
- K. Dong, A. R. Benson, and D. Bindel. Network density of states. In *Proceedings of the 25th ACM SIGKDD International Conference on Knowledge Discovery & Data Mining*, KDD '19, pages 1152–1161. ACM, 2019.
- G. Elsayed, D. Krishnan, H. Mobahi, K. Regan, and S. Bengio. Large margin deep networks for classification. In *Advances in Neural Information Processing Systems*, pages 842–852, 2018.
- A. Fawzi, S.-M. Moosavi-Dezfooli, P. Frossard, and S. Soatto. Empirical study of the topology and geometry of deep networks. In *Proceedings of the IEEE Conference on Computer Vision and Pattern Recognition*, pages 3762–3770, 2018.
- G. H. Golub and C. F. Van Loan. *Matrix Computations*. JHU Press, Baltimore, 4th edition, 2012.
- Y. Guo and D. Schuurmans. Discriminative batch mode active learning. In *Advances in Neural Information Processing Systems*, pages 593–600, 2008.
- K. He, X. Zhang, S. Ren, and J. Sun. Identity mappings in deep residual networks. In *European conference on computer vision*, pages 630–645. Springer, 2016.
- A. Katharopoulos and F. Fleuret. Not all samples are created equal: Deep learning with importance sampling. In *International Conference on Machine Learning*, pages 2530–2539, 2018.
- B. Kim, C. Rudin, and J. A. Shah. The bayesian case model: A generative approach for case-based reasoning and prototype classification. In *Advances in Neural Information Processing Systems*, pages 1952–1960, 2014.
- P. W. Koh and P. Liang. Understanding black-box predictions via influence functions. In *International Conference on Machine Learning (ICML 2017)*, pages 1885–1894, 2017.
- P. W. Koh, K.-S. Ang, H. H. Teo, and P. Liang. On the accuracy of influence functions for measuring group effects. *arXiv preprint arXiv:1905.13289*, 2019.
- A. Krizhevsky, G. Hinton, et al. Learning multiple layers of features from tiny images. Technical report, Cite-seer, 2009.
- G. Kutyniok and D. Labate. *Shearlets: Multiscale analysis for multivariate data*. Springer Science & Business Media, 2012.
- A. Lapedriza, H. Pirsiavash, Z. Bylinskii, and A. Torralba. Are all training examples equally valuable? *arXiv preprint arXiv:1311.6510*, 2013.
- O. Li, H. Liu, C. Chen, and C. Rudin. Deep learning for case-based reasoning through prototypes: A neural network that explains its predictions. In *Proceedings of AAAI Conference on Artificial Intelligence*, 2018.
- S. Lloyd. Least squares quantization in PCM. *IEEE Transactions on Information Theory*, 28(2):129–137, 1982.
- I. Loshchilov and F. Hutter. Online batch selection for faster training of neural networks. *arXiv preprint arXiv:1511.06343*, 2015.
- P. Meletis, R. Romijnders, and G. Dubbelman. Data selection for training semantic segmentation CNNs with cross-dataset weak supervision. *arXiv preprint arXiv:1907.07023*, 2019.
- H. Noh, A. Araujo, J. Sim, T. Weyand, and B. Han. Large-scale image retrieval with attentive deep local features. In *Proceedings of the IEEE International Conference on Computer Vision*, pages 3456–3465, 2017.
- L. Ohno-Machado, H. S. Fraser, and A. Ohn. Improving machine learning performance by removing redundant cases in medical data sets. In *Proceedings of the AMIA Symposium*, page 523. American Medical Informatics Association, 1998.
- R. Reisenhofer, S. Bosse, G. Kutyniok, and T. Wiegand. A haar wavelet-based perceptual similarity index for image quality assessment. *Signal Processing: Image Communication*, 61:33–43, 2018.
- M. P. Sampat, Z. Wang, S. Gupta, A. C. Bovik, and M. K. Markey. Complex wavelet structural similarity: A new image similarity index. *IEEE Transactions on Image Processing*, 18(11):2385–2401, 2009.
- K. A. Sankararaman, S. De, Z. Xu, W. R. Huang, and T. Goldstein. The impact of neural network overparameterization on gradient confusion and stochastic gradient descent. *arXiv preprint arXiv:1904.06963*, 2019.
- P. Tschandl, C. Rosendahl, and H. Kittler. The ham10000 dataset, a large collection of multi-source dermatoscopic images of common pigmented skin lesions. *Scientific data*, 5:180161, 2018.
- H. V. Vo, F. Bach, M. Cho, K. Han, Y. LeCun, P. Pérez, and J. Ponce. Unsupervised image matching and object discovery as optimization. In *Proceedings of the IEEE Conference on Computer Vision and Pattern Recognition*, pages 8287–8296, 2019.
- K. Vodrahalli, K. Li, and J. Malik. Are all training examples created equal? An empirical study. *arXiv preprint arXiv:1811.12569*, 2018.
- U. von Luxburg. A tutorial on spectral clustering. *Statistics and Computing*, 17(4):395–416, 2007.

- Z. Wang and E. P. Simoncelli. Translation insensitive image similarity in complex wavelet domain. In *Proceedings of IEEE International Conference on Acoustics, Speech, and Signal Processing*, volume 2, pages 573–576. IEEE, 2005.
- Z. Wang, A. C. Bovik, H. R. Sheikh, E. P. Simoncelli, et al. Image quality assessment: From error visibility to structural similarity. *IEEE transactions on image processing*, 13(4):600–612, 2004.
- R. Yousefzadeh. *Interpreting Machine Learning Models and Application of Homotopy Methods*. PhD thesis, University of Maryland, College Park, 2019.
- R. Yousefzadeh and D. P. O’Leary. Interpreting neural networks using flip points. *arXiv preprint arXiv:1903.08789*, 2019a.
- R. Yousefzadeh and D. P. O’Leary. Investigating decision boundaries of trained neural networks. *arXiv preprint arXiv:*, 2019b.
- R. Yousefzadeh and D. P. O’Leary. Refining the structure of neural networks using matrix conditioning. *arXiv preprint arXiv:*, 2019c.
- J. Zujovic, T. N. Pappas, and D. L. Neuhoff. Structural texture similarity metrics for image analysis and retrieval. *IEEE Transactions on Image Processing*, 22(7):2545–2558, 2013.